

Methodology Article

Comparative Study of the Voltage Stability of an Hight Voltage Power Grid: Case of the Power Grid of the Electric Community of Benin

Yao Bokovi*, Comlanvi Adjmagbo, Adekunle Akim Salami, Ayite Sena Akoda Ajavon

Department of Electrical Engineering, National School of Engineers (ENSI), Regional Center of Excellence for the Control of Electricity (CERME), University of Lomé (UL), Lomé, Togo

Email address:

bokoviyao@gmail.com (Y. Bokovi), adjmagbonicolas@yahoo.fr (C. Adjmagbo), akim_salami@yahoo.fr (A. A. Salami), asajavon@yahoo.fr (A. S. A. Ajavon)

*Corresponding author

To cite this article:

Yao Bokovi, Comlanvi Adjmagbo, Adekunle Akim Salami, Ayite Sena Akoda Ajavon. Comparative Study of the Voltage Stability of an Hight Voltage Power Grid: Case of the Power Grid of the Electric Community of Benin. *Science Journal of Energy Engineering*. Vol. 8, No. 2, 2020, pp. 15-24. doi: 10.11648/j.sjee.20200802.11

Received: August 4, 2020; **Accepted:** August 24, 2020; **Published:** September 7, 2020

Abstract: The voltage profile at the buses of an hight voltage power grid makes it possible to predict the voltage stability of said power grid in order to guarantee production-consumption adequacy. The study presented in this paper is initially restricted to the variation of the active power demand of a consumption bus (PQ) in order to obtain the voltage profile of the entire electricity transmission network. Then, it makes it possible to predict the limit of the maximum increase in power demand at a PQ bus with the corresponding voltage level of all the other buses in order to anticipate the instability of the voltages liable to cause the collapse of the network. Finally, to correct the voltage levels linked to the observed instability, the study proposes the comparison by voltage sensitivity factors of two types of compensation such as shunt compensation and compensation by adding reactance to the line. transmission. The Newton-Raphson method coupled with Predictor-Corrector methods was used for the Continuation Power Flow (CPF) on the electricity transmission network of the Benin Electric Community (CEB). The results from the bus voltage profile curves for the case of the CEB power grid have shown that the two types of compensation make it possible to recover the lost voltage stability. However, shunt compensation is best due to its lower voltage stability sensitivity factor. This study has the advantage of allowing the power grid operator to anticipate the instability of the tensions in the power grid in order to avoid its collapse. It thus helps the manager to properly plan the voltage stability of his power grid.

Keywords: Continuation Power Flow, Newton-Raphson, Voltage Profile, Shunt Compensation, Transmission Line Reactance, Voltage Stability Sensitivity Factor

1. Introduction

High Voltage (HV) power grid serve as a link between production centers and large areas of electrical energy consumption; these networks are said to be electrical energy transport or even interconnection [1]. They are characterized by buses with which are associated production groups, loads (consumption), lines and electrical energy transformers. This leads to the electrical system consisting of the production,

transport and consumption (loads) of electrical energy, the main objectives of which are the search for quality and the reduction of operating costs while respecting the security constraints of said system. The major safety constraints in an HV power grid are the stability limit and the voltage profile [2].

Stability is linked to the power transit capacity of the

transmission lines [3, 4]. The profile of the voltages at the power grid buses makes it possible to evaluate the variation in the voltage of each bus of the network in order to control the stability of the said power grid within its limits to guarantee a production - consumption adequacy [5]. Several studies have been done on voltage stability based on repeated analyzes of the power flow (PF) with the Newton-Raphson method [6]. The major difficulty of this method is the Jacobian matrix of Newton-Raphson which becomes singular at the critical point of the limit of stability in tension; which leads to an error and a divergence in the solution of the power flow at the critical point, [6, 7, 8]. To remedy these shortcomings, we reformulate the PF equations by applying a local technique of continuous parameterization called Continuation Power Flow (CPF) [6, 9]. The CPF method makes it easy to study the voltage stability of electrical systems as in several studies [6, 10, 12]. The stability of the power grid using the CPF after insertion of a wind power plant in said grid has been studied in [11]. CPF was used in [12] to simulate the near-stable state of an electrical system. In [13], it developed the simulation of dynamic load restoration using CPF. (ZHAO & al. 2015) contributed in [10] from CPF to the study of voltage stability according to the evolution of the load at the border between the transmission network and the energy distribution network electric. Sudden drops in voltage at buses in an power grid have been investigated in [14] using the CPF. These studies are aimed at preventing voltage instability due to increased demand for electrical energy, which could lead to the collapse of power grid. Avoiding the collapse of power grid implies finding a solution for restoring voltage stability, hence the compensation measures or at worst the shedding of certain loads. There are several compensation modes [9] among which we can cite Generator AVR's, Under-Load Tap Changers, Shunt Capacitors, Series Capacitors, Shunt Reactors, Synchronous Condensers.

In this paper, the objective is to predict not only the limit of the maximum increase in power demand at a PQ bus but also the voltage instability in order to provide an acceptable compensation. Two compensation modes such as Shunt Capacitors and Series Capacitors are presented and compared for the case of the CEB's HV power grid. For the choice of the appropriate compensation mode, it was first carried out to vary the active power demand of a PQ consumption bus in order to obtain the voltage profile of the entire electricity transmission network. Then, the limit of the maximum increase in power demand at the PQ bus with the corresponding voltage level of all other buses was predicted in order to anticipate the instability of the voltages that could cause the grid to collapse. Finally, the correction of the voltage levels linked to the observed instability, is obtained through compensations such as shunt compensation and compensation by adding reactance to the transmission line with the determination of their voltage sensitivity factors. The study presented in this paper is based on the Newton-Raphson method coupled with the Predictor-Corrector methods used for Continuation Power Flow (CPF). So this paper is structured as follows. After the

introduction, we first explain the CPF method used, followed by the presentation of the CEB's HV power grid. Then the data processing with the results is carried out and finally the analyzes and discussions are presented followed by the conclusion.

2. The Continuation Power Flow Method: CPF

The CPF method begins with the basic conditions using conventional solutions of load distribution (Load Flow: LF) from the Newton-Raphson algorithm to calculate the basic parameter denoted λ . To do this, we reformulate the Load Flow equation to introduce a load parameter λ . We rewrite the Load Flow equation in a matrix form known as the Jacobian matrix J.

Consider the conventional Load Flow equation defined in relation (1), [14].

$$\begin{bmatrix} P_i - P_{gi} + P_{Li} \\ Q_i - Q_{gi} + Q_{Li} \end{bmatrix} = 0 \quad (1)$$

avec:

$$P_i = \sum_{k=1}^n V_i V_k Y_{ik} \cos(\delta_i - \delta_k - \theta_{ik}) \quad (2)$$

$$Q_i = \sum_{k=1}^n V_i V_k Y_{ik} \sin(\delta_i - \delta_k - \theta_{ik}) \quad (3)$$

where: P_i and Q_i are respectively the active and reactive powers at node i ; P_{gi} and Q_{gi} the active and reactive powers generated at node i ; P_{Li} and Q_{Li} the active and reactive power consumed at the bus i ; $V_i \angle \delta_i$ and $V_k \angle \delta_k$ the voltages at buses i and k ; $Y_{ik} \angle \theta_{ik}$ the admittance (i, k) element of the Ybus admittance matrix; n is the total number of buses in the power grid.

By asking $P_i^{inj} = P_{gi} - P_{Li}$ and $Q_i^{inj} = Q_{gi} - Q_{Li}$, we rewrite relation (1) in relation (4).

$$g(\delta, V) = \begin{bmatrix} P(\delta, V) - P^{inj} \\ Q(\delta, V) - Q^{inj} \end{bmatrix} = 0 \quad (4)$$

where: $P(\delta, V)$ and $Q(\delta, V)$ are the vectors of the active and reactive power of the power grid; (δ, V) variable vector composed of the angle and the magnitude of the voltage of each bus of the power grid; P^{inj} and Q^{inj} are the vectors of the active and reactive power injected from each bus of the network.

In order to know the state of the electrical system for different load factors, we must add a state variable λ to equation (4); we can obtain the plot of δ "and" V by varying λ [7]. The system of equation (4) then becomes that of relation (5).

$$f(\delta, V, \lambda) = \begin{bmatrix} P(\delta, V) - \lambda P^{inj} \\ Q(\delta, V) - \lambda Q^{inj} \end{bmatrix} = 0 \quad (5)$$

where: λ is the continuous parameter such that $0 \leq \lambda \leq \lambda_{max}$.

In the Newton-Raphson method (method not developed in this paper) for Load Flow, the reformulated Jacobian matrix of

the system of equations (5) is written at relation (6), [7].

$$J(\delta, V, \lambda) = \begin{pmatrix} \frac{\partial P_2}{\partial \delta_2} & \dots & \frac{\partial P_2}{\partial \delta_n} & \frac{\partial P_2}{\partial V_{m+2}} & \dots & \frac{\partial P_2}{\partial V_n} & \frac{\partial P_2}{\partial \lambda} \\ \vdots & & \vdots & \vdots & & \vdots & \vdots \\ \frac{\partial P_n}{\partial \delta_2} & \dots & \frac{\partial P_n}{\partial \delta_n} & \frac{\partial P_n}{\partial V_{m+2}} & \dots & \frac{\partial P_n}{\partial V_n} & \frac{\partial P_n}{\partial \lambda} \\ \frac{\partial Q_{m+2}}{\partial \delta_2} & \dots & \frac{\partial Q_{m+2}}{\partial \delta_n} & \frac{\partial Q_{m+2}}{\partial V_{m+2}} & \dots & \frac{\partial Q_{m+2}}{\partial V_n} & \frac{\partial Q_{m+2}}{\partial \lambda} \\ \vdots & & \vdots & \vdots & & \vdots & \vdots \\ \frac{\partial Q_n}{\partial \delta_2} & \dots & \frac{\partial Q_n}{\partial \delta_n} & \frac{\partial Q_n}{\partial V_{m+2}} & \dots & \frac{\partial Q_n}{\partial V_n} & \frac{\partial Q_n}{\partial \lambda} \end{pmatrix} \quad (6)$$

This Jacobian matrix makes it possible to find the point of bifurcation of the system by systematic gradual increase of the load factor λ of the system thanks to the CPF. CPF techniques are a very robust tool for the calculation of trajectories of one or more parameters [7]. The considered system is summarized by relation (5).

Continuation Power Flow (CPF) is an iterative process which from an initial solution defined by $(\delta^j, V^j, \lambda^j)$, consist to calculate a new situation $(\delta^{j+1}, V^{j+1}, \lambda^{j+1})$ with $\lambda^j > \lambda^{j+1}$. This process thus converges towards λ_{max} .

The CPF is then carried out in three steps, namely parametrization, prediction and correction.

2.1. Parametrization

Parametrization is mathematically a means of identifying each solution so that the next or previous solution can be evaluated. In this paper, the natural parametrization which takes directly λ as a parameter has been used according to relation (7).

$$p^j(\delta, V, \lambda) = \lambda - \lambda^j - \sigma = 0 \quad (7)$$

where: λ^j is the initial parameter; λ the new parameter and σ continuous measurement of the step.

2.2. Prediction

Prediction is the process of producing an estimate

$(\delta^{j+1}, V^{j+1}, \lambda^{j+1})$ of the new solution according to relation (8).

$$\begin{bmatrix} \delta^{j+1} \\ V^{j+1} \\ \lambda^{j+1} \end{bmatrix} = \begin{bmatrix} \delta^j \\ V^j \\ \lambda^j \end{bmatrix} + \sigma \bar{z}_j \quad (8)$$

with:

$$\bar{z}_j = \frac{z_j}{\|z_j\|_2} \quad (9)$$

$$\begin{bmatrix} f_\delta & f_V & f_\lambda \\ e_k \end{bmatrix} z_j = \begin{bmatrix} 0 \\ 1 \end{bmatrix} \quad (10)$$

where: $z_j = [d\delta \, dV \, d\lambda]$ is the tangent vector; \bar{z}_j is the normalized tangent vector; $e_k = [p_\delta^{j-1} \, p_V^{j-1} \, p_\lambda^{j-1}]$ is the appropriate and dimensioned row vector such that all its elements are zero except the $k^{i\text{eme}}$ element that is worth ± 1 the sign of the variation; k is the index of the maximum component of the tangent vector respecting the relation (11), [14].

$$(\delta_k, V_k) : |z_k| = \max \{|z_1|, |z_2|, \dots, |z_N|\} \quad (11)$$

where: $N=2n_1 + n_2 + 1$ with n_1 the number of buses PQ and n_2 the one of generation buses PV.

Table 1. The data of the CEB's HV power grid buses.

a	b	c	d	e	f	g	h	i	j	k	l	m	n
VRA	1	3	0	0	0	0	1	1	0	161	1	1.3	0.9
ATA	2	1	3.9	2.8	0	0	1	1	0	161	1	1.3	0.9
AVA	3	1	2.6	1.59	0	0	1	1	0	161	1	1.3	0.9
BOH	4	1	6.5	4.5	0	0	1	1	0	161	1	1.3	0.9
CVE	5	1	36.6	17.89	0	0	1	1	0	161	1	1.3	0.9
KAR	6	1	7.745	3.786	0	0	1	1	0	161	1	1.3	0.9
LAF	7	1	37.17	18.172	0	0	1	1	0	161	1	1.3	0.9
LPO	8	2	21.23	12.99	0	0	1	1	0	161	1	1.3	0.9
MAG	9	2	0	0	0	0	1	1	0	161	1	1.3	0.9
MOM	10	1	9.186	5.92	0	0	1	1	0	161	1	1.3	0.9
NAN	11	2	0	0	0	0	1	1	0	161	1	1.3	0.9
ONI	12	1	2.9	5.7	0	0	1	1	0	161	1	1.3	0.9
SAK	13	1	0.6	0.3	0	0	1	1	0	161	1	1.3	0.9

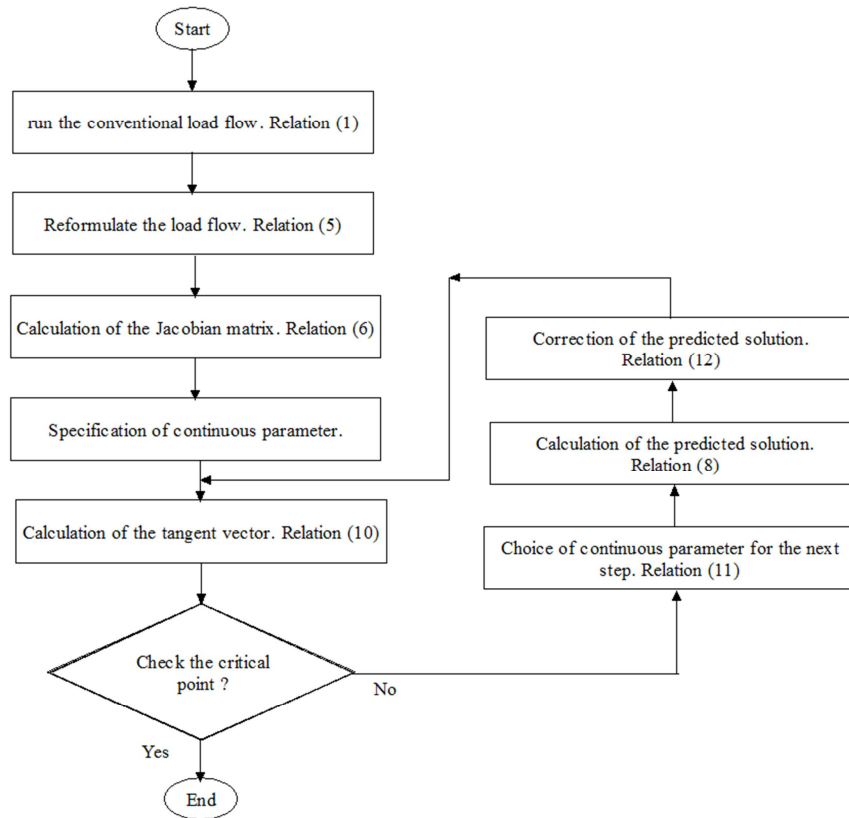


Figure 1. Principle of Continuation power flow.

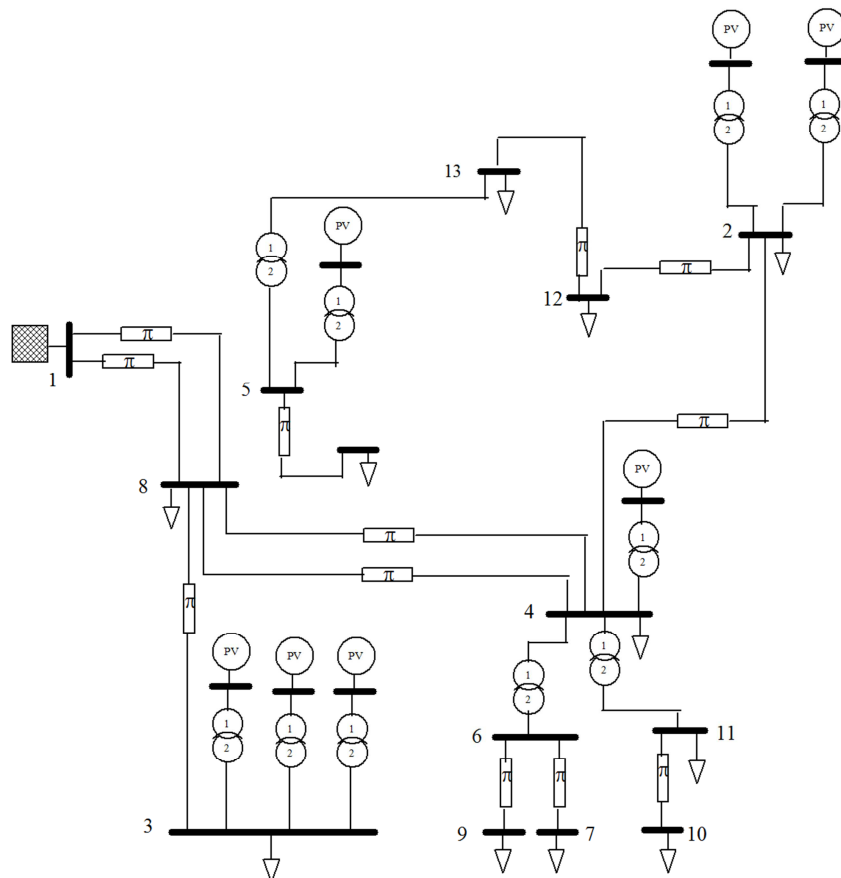


Figure 2. CEB's HV power grid.

2.3. Correction

The correction step provides the new solution $(\delta^{j+1}, V^{j+1}, \lambda^{j+1})$ by correcting the predicted solution $(\hat{\delta}^j, \hat{V}^j, \hat{\lambda}^j)$. The Newton-Raphson method is used to find this new solution by solving the equation system of relation (12).

$$\begin{bmatrix} f(\delta, V, \lambda) \\ p^j(\delta, V, \lambda) \end{bmatrix} = 0 \quad (12)$$

The principle of Continuation power flow is shown in Figure 1.

3. Materials

The CEB's HV power grid shown in Figure 2 and made up of 13 buses and 14 power transmission lines is used in this paper. Matpower 6.0 [15] software in a Matlab R2016a environment was used.

The data from the HV power grid were processed and

modeled according to the format of Matpower, [15, 16]. The data of the CEB's HV power grid buses are presented in table 1.

Legend of table 1. ATA: Atakpamé; AVA: Avakpa; BOH: Bohicon; CVE: Cotonou-Vedogou; KAR: Kara; LAF: Lomé-Aflao; LPO: Lomé-Port; MAG: Maria-Gleta; MOM: Mome-hagou; ONI: Onigbo, SAK: Sakete; a: Design; b: Bus type (1=PQ, 2=PV, 3=Slack, 4=isolated); c: bus number (positive integer); d: real power demand Pd [MW]; e: reactive power demand Qd [MVar]; f: shunt conductance Gs (MW demanded at V=1.0 p.u.); g: shunt susceptance Bs (MVar injected at V=1.0 p.u.); h: area number (positive integer); i: voltage magnitude Vm (p.u.); j: voltage angle Va (degrees); k: base voltage (kV); l: loss zone (positive integer); m: maximum voltage magnitude Vmax (p.u.); n: minimum voltage magnitude Vmin (p.u.).

The buses are distributed as follows: 03 PV bus, 01 slack bus and 09 PQ bus.

Table 2 contains the formatted data of the electrical energy transmission lines of the CEB's HV network.

Table 2. Data of the transmission lines of the CEB's HV power grid.

1	2	3	4	5	6	7	8	9	10	11	12	13
9	13	0.029	0.086	0.040	404	444	485	0	0	1	-360	360
12	13	0.024	0.742	0.034	404	445	485	0	0	1	-360	360
5	9	0.007	0.017	0.007	405	446	486	0	0	1	-360	360
3	9	0.029	0.061	0.026	406	446	487	0	0	1	-360	360
9	10	0.651	0.149	0.065	406	446	487	0	0	1	-360	360
3	10	0.038	0.087	0.038	406	447	487	0	0	1	-360	360
7	10	0.039	0.090	0.039	407	447	488	0	0	1	-360	360
10	11	0.613	0.183	0.084	407	448	488	0	0	1	-360	360
7	8	0.009	0.027	0.012	407	448	489	0	0	1	-360	360
2	6	0.126	0.377	0.171	408	449	490	0	0	1	-360	360
2	11	0.019	0.057	0.026	409	449	490	0	0	1	-360	360
4	11	0.042	0.126	0.058	409	450	491	0	0	1	-360	360
4	12	0.039	0.118	0.054	409	450	491	0	0	1	-360	360
7	1	0.091	0.208	0.091	408	449	490	0	0	1	-360	360

Legend of table 2. 1: F_BUS " from" bus number; 2: T_BUS " to" bus number; 3: BR_R resistance (p.u.); 4: BR_X reactance (p.u.); 5: BR_B total line charging susceptance (p.u.); 6: RATE_A MVA rating A (long term rating), set to 0 for unlimited; 7: RATE_B MVA rating B (short term rating), set to 0 for unlimited; 8: RATE_C MVA rating C (emergency rating), set to 0 for unlimited; 9: TAP transformer off nominal turns ratio, (taps at " from" bus, impedance at " to" bus, i.e. if r=x=b=0, tap=|Vf /Vt|); 10: SHIFT transformer phase shift angle (degrees), positive) delay; 11: BR_STATUS initial branch status, 1=in-service, 0=out-of-service; 12: ANGMIN minimum angle difference, $\theta_f - \theta_t$ (degrees); 13: ANGMAX maximum angle difference, $\theta_f - \theta_t$ (degrees).

4. Methodology

The adopted compensation comparison methodology is presented in Figure 3. In this methodology, we define at each load bus i PQ the sensitivity factor S_{Vi} of the voltage stability by equation (13).

$$S_{Vi} = \left| \frac{dV_i}{dP_{Total}} \right| \quad (13)$$

where dV_i is the variation of the voltage in per unit (pu) at the bus i and dP_{Total} . The lower this sensitivity factor to a bus i compared to another bus j, the more stable the bus i. The voltages of the buses of the power grid are subjected to a constraint of magnitude margin V according to equation 14 to guarantee the stability of the network.

$$V_{min} \leq V \leq V_{max} \quad (14)$$

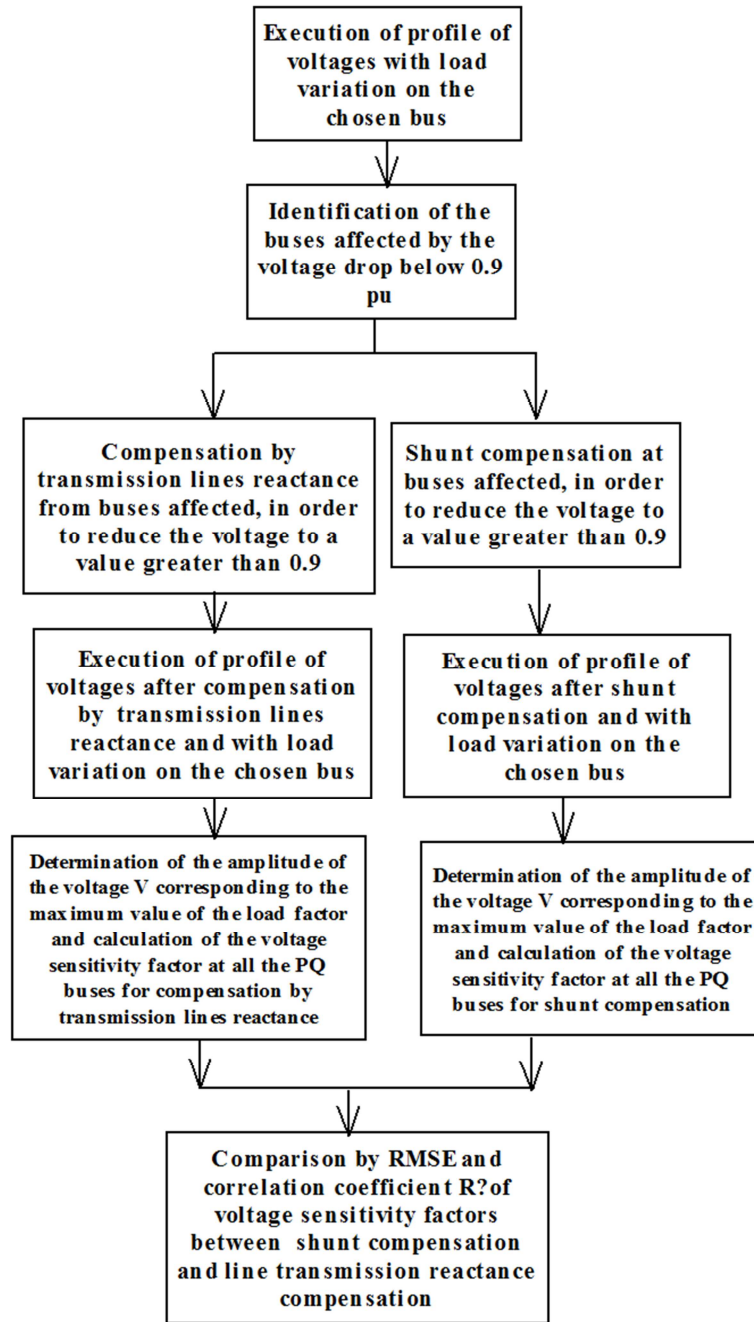


Figure 3. Compensation methodology.

5. Results

By varying the active power demand on bus 6 of the CEB's power grid via the load factor λ , the voltage magnitude of the nine (09) PQ buses is obtained through the network voltage profile. Figure 4 shows the voltage profile.

The critical voltage at bus 6 is 0.5616 pu for a maximum load factor λ_{max} equal to 0.2705. This led to making the two types of compensation, namely the shunt compensation to bus 6 and the compensation by reactance of the transmission line on line (2-6) of the CEB's power grid. Figures 5 and 6 show

the voltage profile curves of the two types of compensation at bus 6.

While respecting the constraints related to the minimum and maximum magnitudes on bus 6, the results retained for the two types of compensation are summarized in Table 3.

Once the two types of compensation have been able to bring the maximum voltage of bus 6 to values greater than 0.9 pu, then we add a shunt of 0.6 pu to bus 6 and we bring back the reactance X_{2-6} of the line (2- 6) to 0.1 X_{2-6} . For each type of compensation with the optimal values in table 3, continuous power flow is carried out to obtain the profile of the voltage

amplitudes of all the PQ buses in the network. Figures 7 and 8 show these profiles.

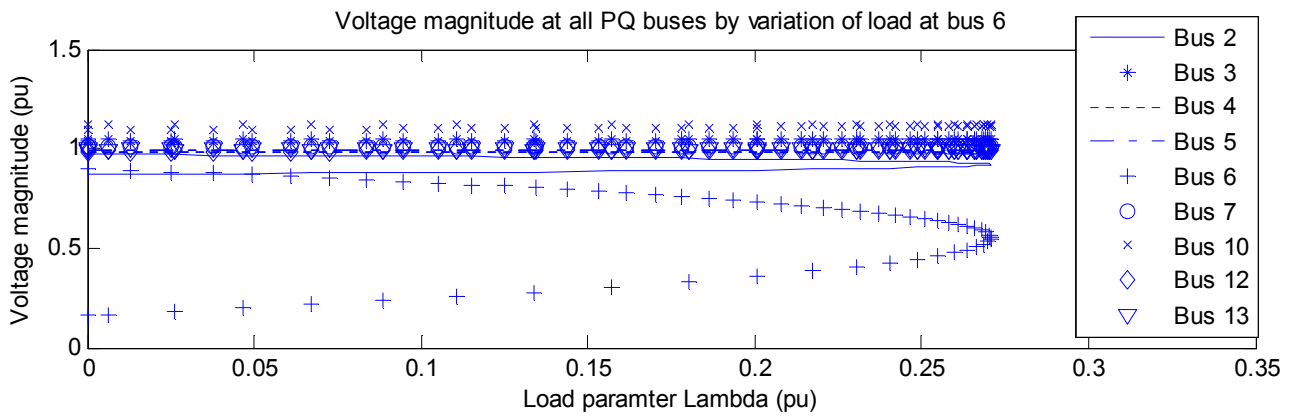


Figure 4. Voltage magnitude at all PQ buses by variation of load at bus 6.

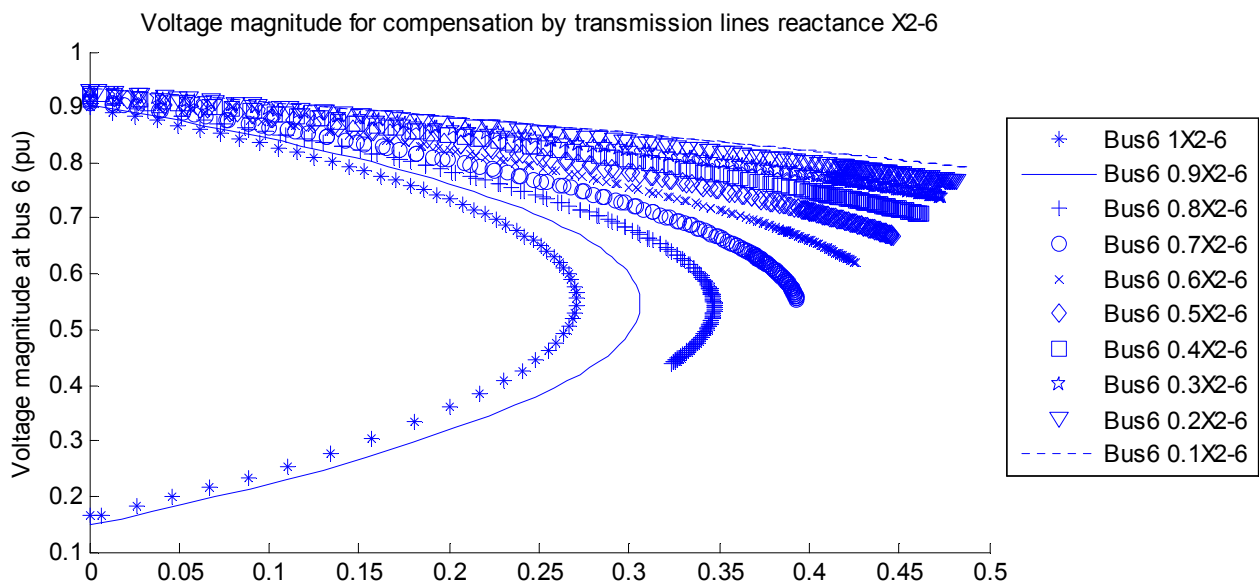


Figure 5. Voltage magnitude at bus 6 with compensation by transmission lines reactance X2-6.

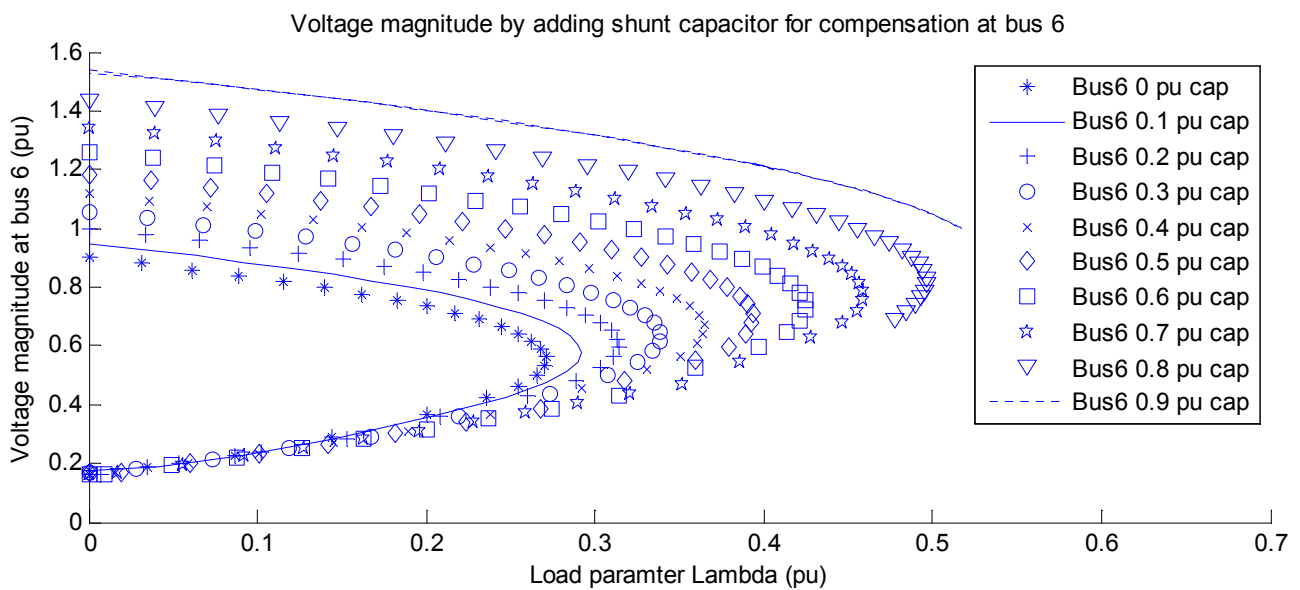
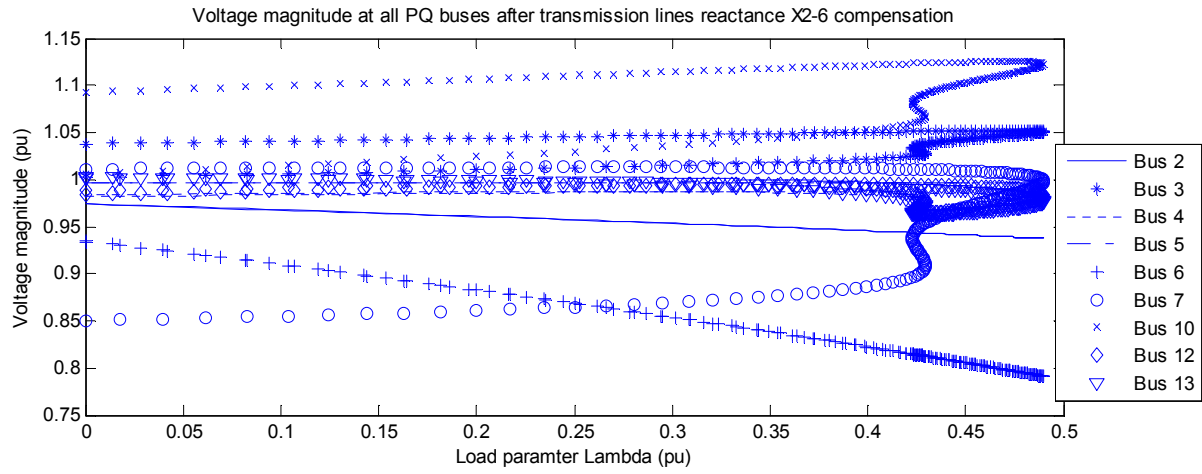
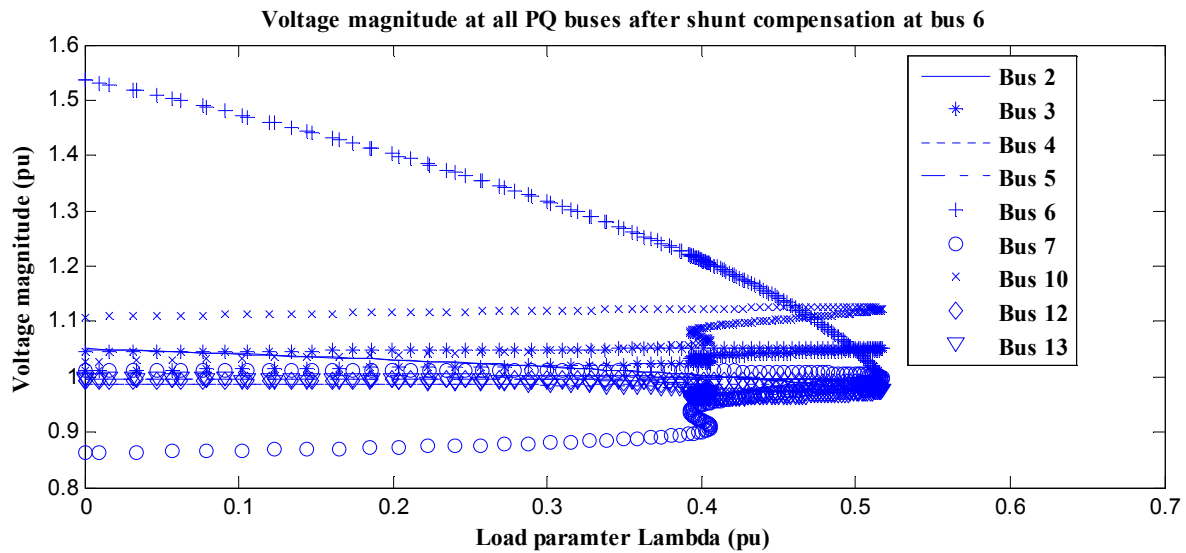


Figure 6. Voltage magnitude by adding shunt capacitors for compensation at bus 6.

Table 3. Results of two types of compensation at bus 6 in CEB's power grid.

Type of compensation	V_{6max} [pu]	$V_{6critical}$ [pu]	Load parameter λ_{max} [pu]	Voltage stability sensitivity factor: Sv_6
Shunt: 0,6 pu	1.25	0.97	0.45	0.010
Line transmission reactance 0.1X2-6	0.95	0.79	0.48	0.011

**Figure 7.** Voltage magnitude at all PQ buses after transmission line reactance X2-6 compensation.**Figure 8.** Voltage magnitude at all PQ buses after shunt compensation at bus 6.

Tables 4 and 5 contain the maximum value of the load parameter λ_{max} with the amplitudes of the corresponding critical voltages $V_{critical}$ and of the sensitivity factor of the voltage stability for each PQ bus of the power grid respectively after the line transmission reactance compensation and the shunt compensation.

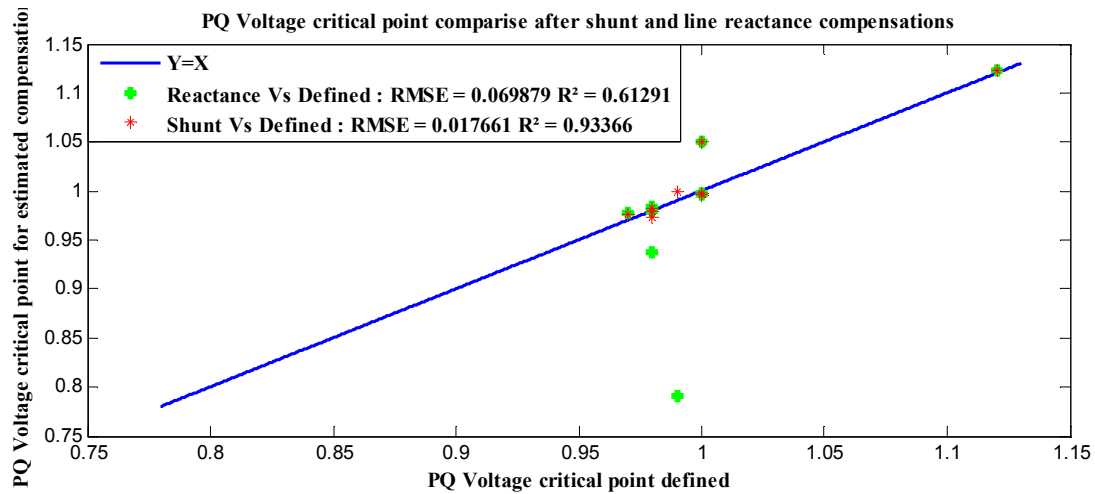
Table 4. New values of critical voltage magnitude and sensitivity factor for all PQ buses after line transmission reactance compensation at bus 6 in CEB's power grid.

$\lambda_{max}=0.489$ pu after line transmission reactance compensation at bus 6		
PQ Bus N°	$V_{critical}$ [pu]	Voltage stability sensistivity factor Sv
2	0.93759	0.00273
3	1.05095	0.00982
4	0.97914	0.00018
5	0.996	2.98E-16
6	0.79134	0.01070
7	0.9984	0.00095
10	1.12264	0.00222
12	0.98336	0.00008
13	0.97716	0.00186

Table 5. New values of critical voltage magnitude and sensitivity factor for all PQ buses after shunt compensation at bus 6 in CEB's power grid.

$\lambda_{\max}=0.4517$ pu after shunt compensation at bus 6		
PQ Bus N°	V_{critical} [pu]	Voltage stability sensitivity factor S_v
2	0.972	0.0014
3	1.05	0.00011
4	0.978	0.00013
5	0.996	1.47E-17
6	0.969	0,01018
7	0.998	0.00028
10	1.122	0.00025
12	0.983	0.00017
13	0.976	0.00041

Figure 9 illustrates the comparison of the consequences of the line transmission reactance compensation of line X_{2-6} and of the shunt compensation of bus 6 on all PQ buses compared to the constraints related to the voltage of each PQ bus of the CEB's power grid.

**Figure 9.** PQ voltage critical point compare after shunt and line transmission reactance compensation.

6. Discussion

The increase in the active power demand on bus 6 of the CEB power grid to the critical point reduced the voltage of this bus to 0.5616 pu for a maximum load factor λ_{\max} equal to 0.2705 as shown in Figure 4.

The constraint linked to the voltage of each bus being $0.9 \leq V \leq 1.3$ and presented in table 1 to make the line transmission reactance compensation on line X_{2-6} (Figure 5) and the shunt compensation on bus 6 (Figure 6) in order to bring the bus voltage back within the above mentioned range. The results from these two types of compensation (Table 3) sufficiently show the advantage of shunt compensation on the line transmission reactance by their voltage variation interval which is respectively $0.79 \leq V \leq 0.95$ and $0.95 \leq V \leq 1.25$. The voltage stability sensitivity factor S_{v6} confirms this advantage at its value for the shunt compensation which is 0.010 against 0.011 for the line transmission reactance compensation. However, the maximum load factor λ_{\max} has increased in value in the two compensation cases with 0.45 pu for the shunt compensation against 0.48 pu for the line transmission reactance compensation and this increases the demand for active power.

The evaluation of the repercussions of each of the two types

of compensation made separately in the entire CEB's power grid and presented in Figures 7 and 8 with tables 4 and 5 clearly expresses the acceptable values of the critical voltage amplitude. V_{critical} to all PQ buses except bus 6 (0.79134 pu) for line transmission reactance compensation. Figure 9 indicates for the critical voltages V_{critical} that the values of the RMSE and of the correlation coefficient R^2 of the shunt compensation equal to 0.017661 and 0.93366 are clearly better than those of the line transmission reactance compensation respectively 0.069879 and 0.61291. The sensitivity factors of the voltage stability S_v of the shunt compensation are lower than those of the line transmission reactance to all the PQ buses (Tables 4 and 5).

Thus in this CEB's power grid where the increase in active power demand on bus 6 is noted, shunt compensation offers better voltage stability in view of the results obtained compared to the line transmission reactance.

7. Conclusion

The study proposed in this paper is the comparison of two types of compensation such as shunt compensation and line transmission reactance compensation. These two compensations follow the presence of voltage instability due

to increased demand for active power causing voltage drops to certain buses in the electrical network. The Newton-Raphson method coupled with Predictor-Corrector methods was used for Continuation Power Flow (CPF) on the electricity transmission network of the Benin Electric Community (CEB) to obtain voltage profiles. The results from the node voltage profile curves for the case of the CEB network showed that the two types of compensation make it possible to recover the lost voltage stability and to increase the demand for active power. The load factor λ_{\max} goes from 0.2705 pu to 0.45 pu for the shunt compensation and to 0.48 pu for the line transmission reactance.

For the magnitudes of the critical voltages V_{critical} compared to those of the stresses, the values of the RMSE and of the correlation coefficient R^2 of the shunt compensation are respectively 0.017661 and 0.93366 and are clearly better than those of the line transmission reactance compensation respectively 0.069879 and 0.61291. In addition to this we note that the sensitivity factors of the voltage stability S_v of the shunt compensation are lower than those of the line transmission reactance to all the PQ buses. In short, the stability of the voltages is much more guaranteed by the shunt compensation than the line transmission reactance compensation for the case of the CEB's electrical transmission network. This study will allow the grid operator to predict and anticipate the instability of the voltages in his power grid.

This study allows the manager to anticipate instability and to properly plan compensation for good voltage stability in its power grid.

References

- [1] Bornard Pierre, Pavard Michel, Interconnection and transport networks: adjustment and operation. Engineering techniques, electrical engineering treatise, April 2001.
- [2] SAMI Ammari. Interaction of FACTS devices with dynamic loads in transport and interconnection networks. Doctoral thesis from the National Polytechnic Institute of Grenoble. Specialty in Electrical Engineering. November 2000. MILLER T. J. E.. Reactive power control in Electric System. Ed. John Wiley & sons. 1982.
- [3] Bokovi Yao, Salami Adekunle, Koffi Mawugno Kodjo, Dotche Koffi, Bedja Koffi-Sa. (2019). Comparative study of the voltage drops estimation on electrical distribution grid: Case study of the Togolese Company of Electricity and Energy grid. 19249673, 10.1109/ 2019 IEEE PES/IAS PowerAfrica 2019.8928838. pp 255-260, 2019. DOI: 10.1109/PowerAfrica.2019.8928838.
- [4] LADJICI Ahmed Amine. Evolutionary computing: Application on the optimization of reactive power planning. Master thesis in Electrical Engineering. National Polytechnic School of Alger. Algeria 2005.
- [5] PARUL Anand U. DHURMESHKUMAR P. Voltage Stability assessment using Continuation Power Flow. International Journal of Advanced Research in Electrical, Electronics and instrumentation Engineering. Vol. 2, Issue 8, August 2013. Pp. 4013-4022.
- [6] CASTRO Abad JoséAngel, PHULPIN Yannick. Estimation locale de la stabilité en tension. Conférence EF, ENSEIHT, Toulouse, 6-7 Septembre 2007.
- [7] SOTOMAYOR J. Generic bifurcations of dynamical systems. In dynamical Systems, M. M. Peixoto, Acadeic Press, 1973.
- [8] KESKIN Mehmet B. Continuation Power Flow and Voltage Stability in Power Systems. Thesis M. Sc. Departement of Electrical and Electronics Engineering. Middle east Technical University. USA Sept. 2007.
- [9] ZHAO Jinquan, FAN Xiaolong, LIN Changnian, WEI Wenhui. Distributed continuation power flow method for integrated transmission and active distribution network. J. Mod. Power Syst. Clean Energy: DOI 10. 1007/140565-015-0167-2 2015. Pp. 573-582.
- [10] KUMAR Satish & al. Analysis of Power Flow, Continuous Power Flow and Transient Stability of IEEE-14 Bus integrated Wind Farm Using PSAT. 978-1-4673-7492-7/15. IEEE 2015.
- [11] WANG Q., SONG H., AJJARAPU V.. Continuation-Based Quasi-Steady-State analysis. IEEE trans. On power systems. Vol 21, N°1, Fb. 2006. Pp. 171-179.
- [12] ZHAO Jinquan, WANG Yi. A new Continuation Power Flow Model for simulating time-domain dynamique load restoration. 978-1-4244-4241- 6/09. IEEE 2009.
- [13] VENKATARAMANA Ajjarapu, COLIN Christy. The Continuation Power Flow: a tool for steady state voltage stability analysis. Transactions on Power Systems. Vol. 7 N°1. February 1992. Pp. 416-423.
- [14] Ray D. Zimmerman Carlos E. Murillo-S_anchez, Matpower 6.0 User's manuel, December 16, 2016.
- [15] A. B. Birch_eld, T. Xu, K. M. Gegner, K. S. Shetye, T. J. Overbye, \Grid Structural Characteristics as Validation Criteria for Synthetic Networks," Power Systems, IEEE Transactions on, 2017. D-17.